

FeAl underlayers for CoCrPt thin film longitudinal media

Li-Lien Lee, D. E. Laughlin, and D. N. Lambeth

Data Storage Systems Center, Carnegie Mellon University, Pittsburgh, Pennsylvania 15213

B2 ordered FeAl films with a small, uniform grain size have been produced by rf diode sputter deposition on glass substrates. CoCrPt films grown on FeAl underlayers were found to have the (10 $\bar{1}$ 0) lamellar texture. The in-plane coercivities (H_c) of the CoCrPt/FeAl films are comparable to those of the CoCrPt/Cr films and they can be further improved by inserting a thin Cr intermediate layer between the CoCrPt and the FeAl layers. By employing a MgO seed layer or a (002) textured Cr seed layer, (001) textured FeAl can be obtained. However, the (001) FeAl underlayer only induces a weak (1120) textured CoCrPt. Thus no improvement in H_c over those produced on unseeded FeAl underlayers was observed. © 1997 American Institute of Physics. [S0021-8979(97)36308-7]

Although 30 years has passed since Cr was first used as an underlayer,¹ with only a few modifications it is still widely used for Co based alloy longitudinal thin film media. One of the important reasons for the popularity of Cr is its capability of promoting in-plane c -axis texture in the overlying Co alloy thin films via grain to grain epitaxy. The epitaxial relationships between Co and Cr which are useful for longitudinal media were found to be (11 $\bar{2}$ 0)_{Co}|| (001)_{Cr},² (10 $\bar{1}$ 1)_{Co}|| (011)_{Cr},³ and (10 $\bar{1}$ 0)_{Co}|| (112)_{Cr}.⁴ However, this ability to provide an epitaxy template is not unique to the Cr underlayer. A new group of underlayers with the B2 (CsCl-type) ordered crystal structure has attracted considerable attention lately.^{5,6} The B2 ordered intermetallic phase NiAl with a lattice constant similar to that of the bcc Cr (2.887 Å vs 2.884 Å) has been shown to be a promising underlayer due to its small, uniform grain size and its ability to induce useful crystallographic textures in the Co based alloy thin films. There are many other B2 phases with similar lattice parameters which may be useful as underlayers in magnetic recording media which have not yet been discussed.

The Fe-Al equilibrium phase diagram⁷ shows that the B2 ordered FeAl exists as a single phase over the composition range extending from 34 to ~50 at. % Al. Bulk FeAl phase with the B2 crystal structure has a lattice constant of 2.907 Å,⁸ which is in the proper range to induce epitaxial growth of Co alloys. It has recently been reported by Wang *et al.*⁹ that a (11 $\bar{2}$ 0) textured Co film can be obtained by slow vapor deposition, in ultrahigh vacuum, onto an FeAl (001) single crystal. Although Wang *et al.* did not study the epitaxy of Co with FeAl single crystal substrates of other orientations, we have found that polycrystalline B2 FeAl is a potential candidate for media underlayers in this and other orientations.

This study investigates sputter deposited FeAl films as underlayers for CoCrPt thin films. Seed layer and intermediate layer schemes previously used by the authors^{6,10} to improve the B2 NiAl underlayers have also been investigated for the FeAl underlayers.

All films in this study were prepared by rf diode sputter-

ing in a three-target sputtering system. Multilayered films were deposited sequentially without venting the chamber. The base pressure was 5×10^{-7} Torr or better. All sputtering was performed at room temperature using 3-in.-diam targets at a fixed ac power of 100 W (2.3 W/cm²) and an Ar gas pressure of 10 mTorr. The target to substrate distance was ~1.2 in. All substrates used were 1 in. square, smooth (non-textured) Corning 7059 glass. Substrates were cleaned twice in three separate ultrasonic baths of acetone, 2-propanol and de-ionized water. The sputtering rates were CoCrPt: 13.3 nm/min, FeAl: 11.4 nm/min, Cr: 13 nm/min, and MgO: 4 nm/min.

The in-plane magnetic properties of the films were measured by vibrating sample magnetometry (VSM) with fields

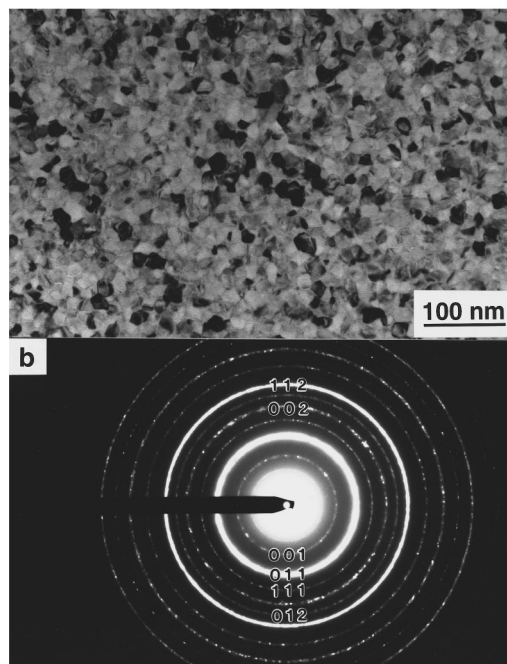


FIG. 1. (a) TEM bright field image and (b) the corresponding electron diffraction pattern of a 100 nm FeAl film.

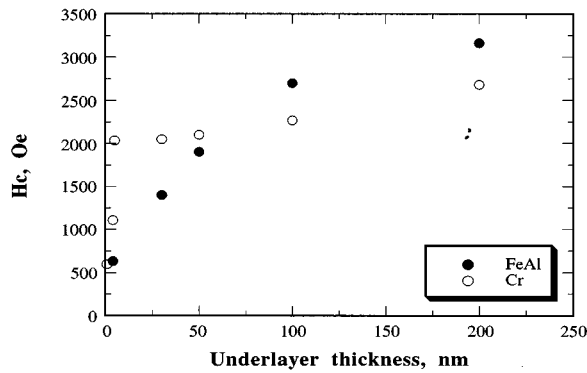


FIG. 2. Comparison of in-plane coercivities (H_c) of 40 nm CoCrPt films on FeAl and Cr underlayers of various thicknesses.

up to 10 kOe. Film structures and compositions were characterized by transmission electron microscopy (TEM) and x-ray diffractometry using Cu K_α radiation and inductively coupled plasma (ICP) atomic emission spectroscopy.

ICP analysis showed that the FeAl film had a composition of 48 at. % Al and 52 at. % Fe; and the CoCrPt film had a composition of 78.5 at. % Co, 9 at. % Cr, and 12.5 at. % Pt. Figure 1 shows the TEM bright field micrograph and the electron diffraction pattern of a 100-nm-thick FeAl film on a glass substrate. The grain size of the film shown in Fig. 1 is estimated to be ~ 15 nm which is similar to that of a B2 NiAl film and smaller than that of a Cr film. The indexed electron diffraction pattern is consistent with that of a B2 structure. This FeAl film is ferromagnetic with low magnetic moment and coercivity ($M_s \sim 17$ emu/cc and $H_c < 2$ Oe), which interferes with the M - H loop of the CoCrPt film. The lattice constant of the FeAl determined from x-ray diffraction of a thick film was found to be 0.290 nm, which is slightly larger than the 0.288 nm of Cr or NiAl. Figure 2 compares the VSM measured in-plane coercivities of the CoCrPt/FeAl and the CoCrPt/Cr films of various underlayer thicknesses. It is found that the in-plane H_c increases progressively as the underlayer thickens for the CoCrPt/FeAl films. This gradual increase of H_c is similar to that of the CoCrPt/NiAl films⁶

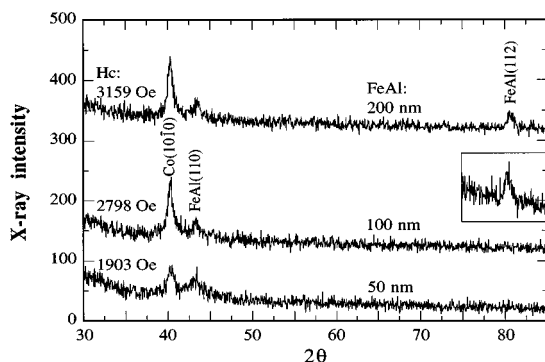


FIG. 3. X-ray diffraction spectra of 40 nm CoCrPt films on 50-, 100-, and 200-nm-thick FeAl underlayers on smooth glass substrates. The inset is a portion of a slow x-ray scan of the film with a 100 nm FeAl underlayer to show the (112) peak.

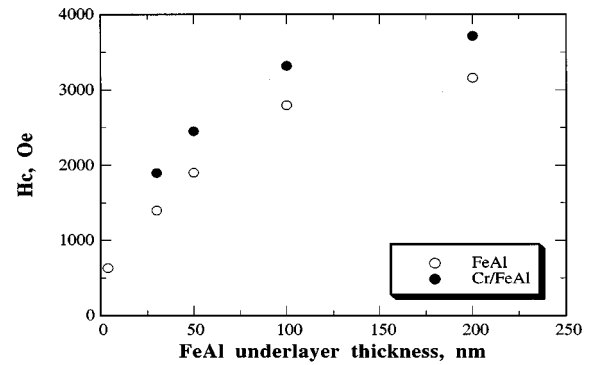


FIG. 4. In-plane coercivities of 40 nm CoCrPt films on various thicknesses of FeAl underlayers with and without 2.5 nm Cr intermediate layers.

but unlike the CoCrPt/Cr films which have a very steep H_c increase in the thin Cr region which then levels off. The H_c of the CoCrPt/FeAl exceeds that of the CoCrPt/Cr as the underlayer becomes thicker than ~ 75 nm. Figure 3 plots the x-ray diffraction spectra of CoCrPt (40 nm) films on FeAl underlayers of 50, 100, and 200 nm thick. The (112) FeAl peak becomes more pronounced as the FeAl thickness increases. The insert is a portion of a slow x-ray scan of the film with a 100 nm FeAl underlayer to bring up the (112) peak. All spectra have $(10\bar{1}0)$ peaks which are indicative of the in-plane c -axis texture of the CoCrPt films. The $(10\bar{1}0)$ peak intensity increases as the (112) peak becomes stronger. Furthermore, we have found that when the CoCrPt/FeAl film is epitaxially grown on a $[110]$ MgO single crystal, the film has only a strong $(10\bar{1}0)/(112)$ texture. This leads us to believe that the $(10\bar{1}0)$ CoCrPt is epitaxially grown on the (112) FeAl. This epitaxy also occurs in a similarly deposited CoCrPt/NiAl film but does not appear in the CoCrPt/Cr film.³ Both the H_c value and the $(10\bar{1}0)$ diffraction peak intensity of the CoCrPt film increase as the FeAl underlayer thickness increases. Although the results reported here are from films deposited on smooth glass substrates, we have also fabricated a few CoCrPt/FeAl films on smooth NiP/Al substrates and they have shown very similar crystallographic textures and coercivities.

When a thin intermediate layer of Cr is inserted between the CoCrPt layer and the FeAl layer, the in-plane coercivity becomes significantly higher. Figure 4 plots the in-plane coercivity of the CoCrPt (40 nm) film versus its FeAl underlayer thickness for films with and without a 2.5 nm Cr intermediate layer. More than a 500 Oe increase in H_c is found for films with the Cr intermediate layers. Our x-ray diffraction studies do not show detectable changes in the crystallographic textures of the CoCrPt/FeAl films with the addition of the Cr intermediate layer.

Since we found that, unlike for Cr films, substrate heating (ranging from 200 to 300 °C) during the deposition was not able to induce a (001) texture in the FeAl films, seed layers were investigated. Both (002) textured Cr and MgO seed layers were studied. Figure 5 shows the x-ray diffraction spectra of two 40-nm-thick CoCrPt films on 100 nm FeAl films with and without a 5 nm Cr seed layer deposited

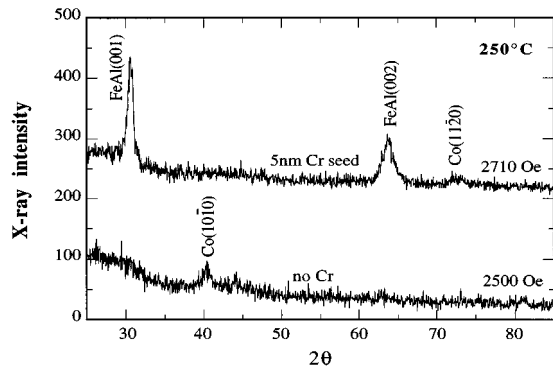


FIG. 5. X-ray diffraction spectra of two CoCrPt (40 nm)/FeAl(100 nm) films on glass substrates with and without a 5 nm Cr seed layer. Both films were deposited with 250 °C substrate preheating.

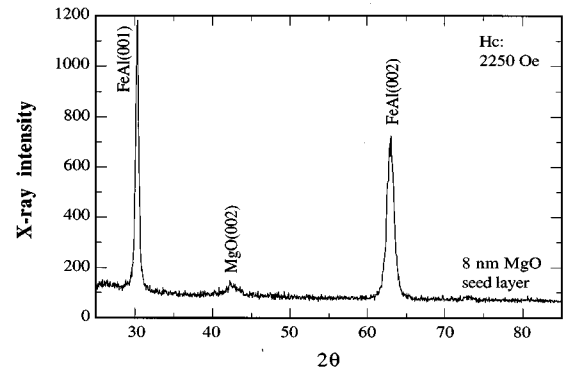


FIG. 6. X-ray diffraction spectrum of a CoCrPt (40 nm)/FeAl (100 nm) film on an 8-nm-thick MgO seed layer on a glass substrate.

prior to the FeAl. In order to induce a (002) texture in the Cr but to have similar temperature induce growth effects, both films were deposited with a 250 °C preheating step. The x-ray spectra are also labeled with their in-plane coercivities. The figure shows that heating alone cannot induce the (001) FeAl texture while the Cr seed layer can. Figure 6 is an x-ray scan of a CoCrPt (40 nm)/FeAl (100 nm) film on an 8-nm-thick MgO seed layer which was deposited without heating onto a glass substrate. It is observed that the MgO seed layer can induce a stronger (001) lamellar texture in FeAl film than can the Cr seed layer. However, the (001) FeAl underlayer suppresses the (1010) texture in the CoCrPt film and only promotes a weak (1120) texture. Thus there is no improvement in the in-plane coercivity over those produced on unseeded and unheated FeAl underlayers.

One final note addresses the ferromagnetism issue of our FeAl underlayers. It is known¹¹ that the intermetallic compound FeAl is nonmagnetic and becomes ferromagnetic as the Fe concentration is increased above 50%. Therefore, sputtered FeAl films can be easily made nonmagnetic if a higher Al concentration is used. However, having a soft-magnetic underlayer with a larger moment may be beneficial. Mallary¹² has patented a longitudinal medium which has an improved cross-talk performance by using a magnetic underlayer to suppress off-track fringing signals. Akiyama *et al.*¹³ have claimed similar results with a soft-magnetic CoFeTa underlayer. The soft-magnetic underlayer can lead to a narrower side written guard band thereby increasing the track density. These investigations have all found that a nonmagnetic buffer layer is needed between the hard magnetic layer and the soft-magnetic underlayer to have adequate control of the balance between the effective head-to-medium magnetostatic coupling and the downward flux leakage from the re-

corded magnetization to the soft-magnetic underlayer. In our case, the Cr intermediate layer can be a good buffer layer with the extra benefit of increase in the coercivity of the media. On the other hand, the soft magnetic FeAl underlayers may also be used to avoid saturation of the magnetoresistance (MR) reading elements by shunting a portion of the magnetic flux.¹⁴ However, further investigation of the recording properties is necessary to elucidate this.

This work is sponsored by the Department of Energy (DOE-FG02-90-ER45423). The facilities used in this study are supported in part by the DSSC of CMU under a grant from the NSF (ECD-89-07068). We also thank Yuichiro Nakamura of the Japan Energy Corporation for supplying the FeAl alloy target.

¹J. P. Lazzari, I. Melnick, and D. Randet, IEEE Trans. Magn. **3**, 205 (1967).

²J. Daval and D. Randet, IEEE Trans. Magn. **6**, 768 (1970).

³G.-L. Chen, IEEE Trans. Magn. **22**, 334 (1986).

⁴K. Hono, B. Wong, and D. E. Laughlin, J. Appl. Phys. **68**, 4734 (1990).

⁵L.-L. Lee, D. E. Laughlin, and D. N. Lambeth, IEEE Trans. Magn. **30**, 3951 (1994).

⁶L.-L. Lee, D. E. Laughlin, and D. N. Lambeth, IEEE Trans. Magn. **31**, 2728 (1995).

⁷U. R. Kattner, in *Binary Alloy Phase Diagrams*, edited by T. B. Massalski (American Society for Metals, Metals Park, OH, 1986), Vol. 1, p. 148.

⁸P. Villars and L. D. Calvert, *Pearson's Handbook of Crystallographic Data for Intermetallic Phases*, 2nd ed. (American Society for Metals, Metals Park, OH, 1991), Vol. 1, p. 815.

⁹C. P. Wang, S. C. Wu, F. Jona, and P. M. Marcus, Phys. Rev. B **49**, 17391 (1994).

¹⁰L.-L. Lee, D. E. Laughlin, and D. N. Lambeth, J. Appl. Phys. **79**, 4902 (1996).

¹¹D. E. Okpalugo, J. G. Booth, and C. A. Faunce, J. Phys. F **15**, 681 (1985).

¹²M. L. Mallary, US Patent No. 5,176,965 (5 January 1993).

¹³J. Akiyama, Y. Ohinata, T. Hikosaka, T. Taguchi, and Y. Tanaka, J. Appl. Phys. **79**, 5655 (1996).

¹⁴M. L. Mallary (private communication).